Al Azhar Bulletin of Science Vol. 29, No. 1 (June) 2018, : pp. 45-58

KINETIC AND THERMODYNAMIC SORPTION STUDY OF COBALT REMOVAL FROM WATER SOLUTION WITH MAGNETIC NANO-HYDROXYAPATITE

A.A. Swelam[1], A.M.A. Salem[2], A.A. Ayman[3], and A.Farghly[4]

[1,2,4]Chemistry Department, Faculty of Science, Al-Azhar University, Cairo, Egypt.
[3]Department of Basic Science, Faculty of Engineering, Modern University for technology & information, Cairo, Egypt

ABSTRACT

In this study, Magnetite–hydroxyapatite nanocomposites were prepared by in situ precipitation of the calcium phosphate phase in an iron oxide colloidal suspension. Adsorption of cobalt was initially rapid and the adsorption process reached a steady state after 180 min. The Co(II) adsorption capability of the MHAp was investigated as a function of temperature, pH, ionic strength, adsorbent dosage, agitation speed and initial Co(II) concentration. Theincrease in pH and temperature resulted in an increase in Co(II) adsorption capacity; Increasing ionic strength increased the adsorption of Co(II) by MHAp; The adsorption isotherms were well described by the Freundlich model, Langmuir, Temkin and D-R models. The Freundlich model was found to provide the better fit with the experimental data. Different types of adsorption kinetic models were used to describe the Co (II) adsorption behaviour, and the experimental results fitted the pseudo-second-order kinetic models well. Thermodynamics parameters such as ΔH^o, ΔS^o, ΔG^o revealed that the adsorption of Co(II) by MHAp was endothermic in nature, physisorption, spontaneous at 308 and 318K.

1. INTRODUCTION

One of the foremost environmental problems existing all around the world is water pollution resulting from the release of industrial effluents. Heavy metal pollution can be found in many industries such as mining operations, metal plating facilities, nuclear power plant, tanneries, petrochemical, metallurgical, electroplating, battery, dying[1], mining and electronic industries. Cobalt is a double-dealing substance with both detrimental and beneficial impact on health. Soil, dust and sea water are regarded as the principal sources of cobalt in the environment. [1,2]. Taking in a little amount of cobalt is necessary for our health due to its inclusion of vitamin B12, but excessive usage of it can be dangerous. Also, a lot of physical and mental problems such as vomiting, nausea, diarrhea, asthma, pneumonia, kidney congestion, skin degeneration and weight loss can be the results of cobalt found in industrial wastewater [3].

In this context, the adsorption combining magnetic separation is one of the most promising technologies. These adsorbents provide an efficient, fast and economical method for separation and remediation studies [4]. By this technique, a mass of wastewater can be disposed in a short time without producing further contaminants [5].We have performed a detailed study of magnetite–hydroxyapatite (Fe_3O_4–HAp) nanocomposites. The effects of contact time, pH, ionic strength and MHAp dose on adsorption processes on the cobalt adsorption, and the adsorption equilibrium andthermodynamic parameters at various Co(II) concentration,temperatures and initial cobalt concentrations were investigated.

2. MATERIALS AND METHODS

2.1. The chemicalsand Adsorbate

All the chemicals ($FeCl_2{\cdot}4H_2O$, $FeCl_3{\cdot}6H_2O$, ammonium hydroxide, HNO_3, KOH, $Ca(NO_3)_2{\cdot}4H_2O$, H_3PO_4 and $CoCl_2$) were of analytical grade supplied by Merck (India). Cobalt chloride stock solutions were prepared by dissolving a desired amount of the metal salt.

2.2. Preparation of cobalt solution

The stock solution (1000 mg/L) of Co (II) was diluted with distilled water to obtain working solutions of varying concentrations for further experiments.

2.3. Preparation of hydroxyapatite (HAp)

The nano-sized hydroxyapatite was prepared by the wet chemical method [6]. First, ammonium hydroxide (25%) was added carefully to 0.25 M phosphoric acid with stirring until we get a solution with pH = 10. Next, 1 M calcium nitrate tetrahydrate solution was mixed slowly with the mixed of phosphoric acid-ammonia solution and stirred vigorously for 1 h. The gel obtained after aging at room temperature for 24 h was dried at 80 °C for another 24 h in a dry oven. The produced (HAp) powder was washed by distilled water several times and sintered for 2 h at 200 °C.

2.4. Preparation of magnetic hydroxyapatite (MHAp)

Briefly, 2g HAp powder was mixed with 80 ml of 1.25 M $FeCl_2 \cdot 4H_2O$ and 2.5 M $FeCl_3 \cdot 6H_2O$ mixture. Then the mixture was purged with nitrogen gas and stirred vigorously at 80 °C. 10 ml of ammonium hydroxide (25%, w/v) was added drop by drop for 30 min. The black product of MHAp was collected by a magnet and washed several times with distilled water and dried in a vacuum oven at 60 °C for 24 h [6].

2.5. Characterization of the prepared samples

Fourier transform infrared (FT-IR) spectra were recorded on a Nicolet IR 200 Fourier transform infrared spectrophotometer (Thermo Scientific Co., USA) with usual KBr pellet technique, using a resolution of 4 cm^{-1} and 16 scans in the range of 400 and 4000 cm^{-1}. Energy Dispersive X-Ray Analysis (EDX) examination of the MHAp were obtained (The samples are examined under EDX microanalyzer –Module Oxford 6587-INCA x-sight attached to Scanning Electron Microscopy (SEM) JEOL-JSM-5500LV scanning electron microscopy at 20KV at the Regional Center of Mycology and Biotechnology, Al-Azhar University, Nasr City, Cairo, Egypt.

2.6. Cobalt removal adsorption experiments

Batch sorption experiments for Co(II) ions removal from aqueous solutions were performed by using the MHAp powder. To run each experiment, 0.1 g of the adsorbent was added to 50 ml of cobalt solution with the desired initial concentration. According to pH of stock solution adjusted by adding proper amounts of 0.1 M HNO_3 or 0.1 M KOH solutions, all sorption experiments were performed at ambient temperature on a magnetic stirrer at 70 rpm, 0.1gMHAp and 50 mL cobalt solution.The Fe_3O_4/HAp composites separate from the solution quickly by a permanent magnet and the clear solution can be easily removed by pipette or decanted off. This simple magnetic separation experiment confirms that Fe_3O_4/HAp composites have magnetic properties and can be used as a magnetic adsorbent to remove pollutants from aqueous solutions [5]. After different interval times of contact, 1 mL of the supernatant solution was withdrawn and diluted with10 mL distilled water. Next, analysed by atomic absorption spectroscopy method (AAS) to determine the remaining cobalt ions concentration.

The adsorption capacities were obtained by mass balance equation.

$$q_e = \frac{(C_o - C_e)}{W \times 100} \times 100 \qquad (1)$$

and the removal percentage (R %) was calculated by the following equation:

The removal percentage yield (R%) =

$$\frac{C_o - C_e}{C_o} \times 100 \qquad (2)$$

where C_o and C_e are initial and equilibrium cobalt ion concentration in solution before and after adsorption process, V (in L) is the solution volume and W (g) is the amount of MHAp adsorbent.

3. RESULTS, DISCUSSION AND CONCLUSION

3.1. Characterization of MHAp

The IR peak at 1046 cm^{-1} originating from phosphate groups of MHAp (Fig.1a) was similar to those observed in natural bone

apatites. Hydroxyl bending peaks of MHAP are identified in 3787 and 470 cm^{-1}. The broad band observed around 3416 cm^{-1} might be ascribed to the O-H stretching vibration on the surface of MHAp component. The band at 574 cm^{-1} isattributed to the Fe-O bond vibration of Fe_3O_4 in MHAp[7]. The characteristic broad absorption mode of a Fe-O group appears in all spectra. Absorption intensity of Fe-O group isdecreased in the three samples, suggesting that the magnetic Fe_3O_4 nanoparticles are successfully embedded into the HAp material. PO_4 peaks at 470, 574 and 1046 cm^{-1} are observed. FTIR data strongly confirm the formation of Fe_3O_4/HAp [8].The FTIR spectrum confirms that the prepared MHApcontained plentiful oxygen functional groups, all these groups could act as available adsorption sites and play an important role in the heavy metal ions removing process and the existence of Fe_3O_4 guaranteed the magnetic properties of materials.Figure 1b show the SEM images of Fe_3O_4/HAp composites. It is found that, the Fe_3O_4/HAp is composed of irregularly shaped particles with the average size of ~120 nm (Fig. 1a).There are obvious peaks of O, Ca, P and Fe in the EDX analysis (Fig. 1c). The peaks of O, Ca and P implie that the presence of Hap and Fe is consistent with Fe_3O_4 and the basic elements of MHAp. This result indicates that HApis successfully anchored on Fe_3O_4.The obvious peaks of these elements indicate that the MHApis synthesized successfully by our proposed method, and it was a proper adsorbent candidate for water treatment. The EDX analysis of cobalt before and after treated MHAp material (Fig. 1d) confirms the existence of cobalt peaks in the spectrum and the percentage of calcium, iron and phosphorus is drastically diminished. This may be due to the removal of calcium, iron and phosphorus by cobalt ions which once again supports the cobalt sorption onto MHAp material.

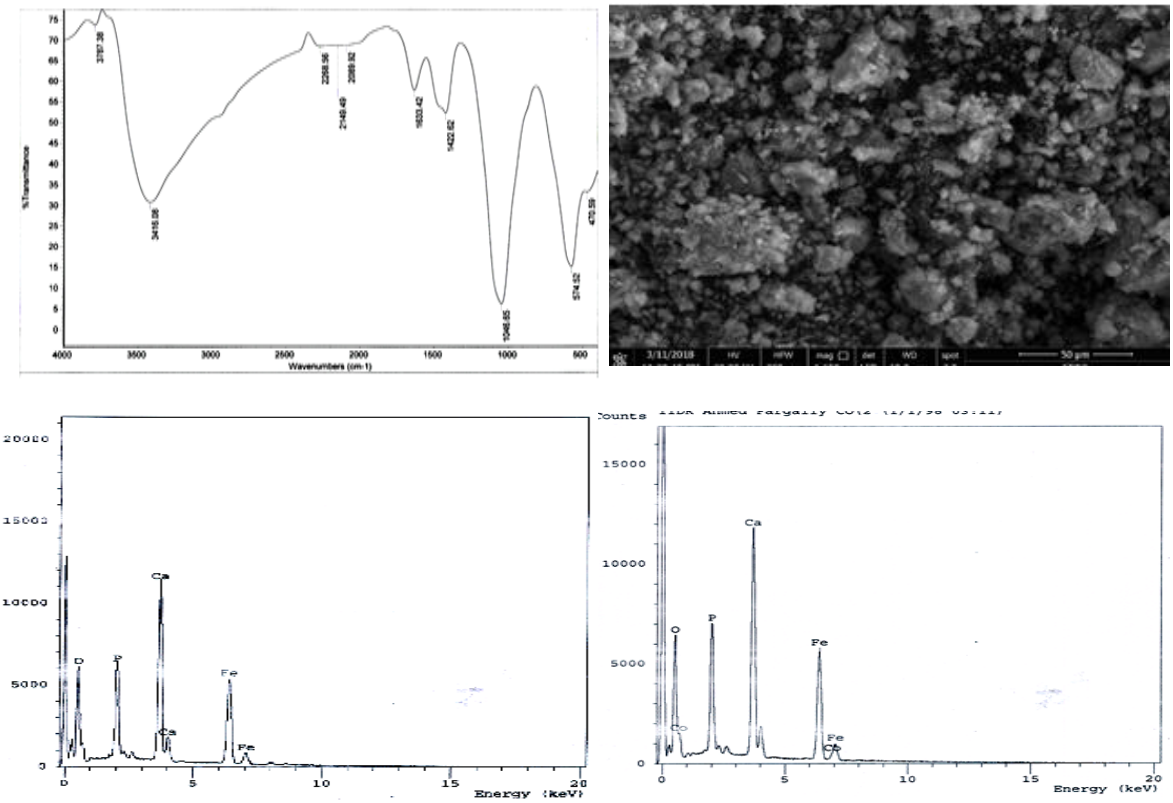

Fig.1. IR plot (a), SEM (b), EDX before adsorption (c), after adsorption (d)

3.2. The effect of the initial Co(II) concentration in the adsorption process

Six different concentrations (4.92, 7, 7.38, 13.16, 20.39 and 28.43 mg/l) were selected to investigate the effect of initial Co(II) concentration (C_o) on the adsorption of cobalt ions onto MHAp adsorbent. It was observed that Co(II) (28.43 mg/l): MHAp adsorbent showed a maximum adsorption capacity compared to other initial concentrations . a plot of the adsorption capacity of Co ions: MHAp with different concentrations at equilibrium in solution was shown in Fig. (2). It reveals that with increase in Co(II) concentration from 4.92 to 28.43 mg/l, the amount of cobalt adsorbed ranged from 2.01to 7.97 mg/g in 180 min. It is clear that the adsorption process is highly dependent on the initial concentration of solution. This increase continues up to 10.34 ppm Co. These results indicate that energetically more favourable sites become involved with increasing Co concentrations in the wastewater solution. Adsorption of Co(II) at a surface site can involve several mechanisms, such as physic-chemical sorption, ion exchange, precipitation or complexation [9].

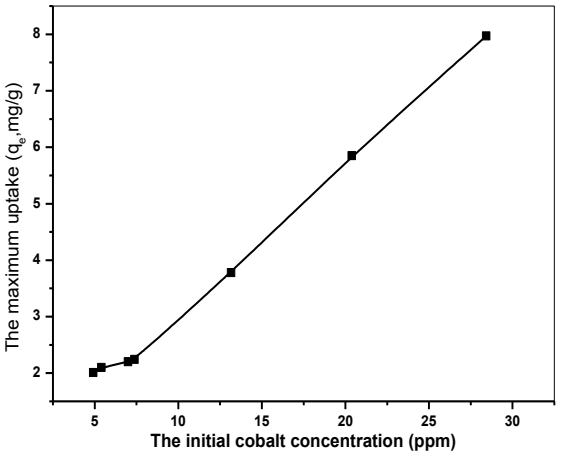

Fig. 2.Effect of initial concentration

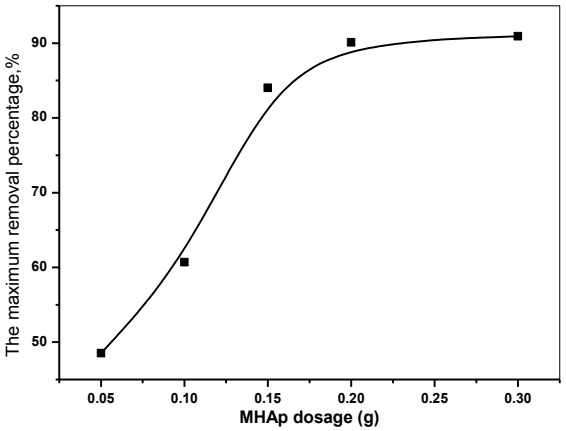

Fig. 3. Effect of the MHAp dose

3.3. Effect of dose

The effect of the MHAp amount on% Co(II) removal is investigated in the range from 0.05 to 0.3 g for the cobalt initial solution concentration (7.38 ppm) at the ambient temperature (20^0C), 3 h adsorption time, 70 rpm shaking speed and at neutral pH (pH ≈ 7). The experimental results in Fig.3 revealed that the % Co ions removal increases from 48.51to 90.92 % when the adsorbent dose is increased from 0.05 to 0.3 g. This may be attributed to the increased adsorbent surface area, pores, active sites and the number of unsaturated sites [10]. According to these parameter values, cobalt ion will have a greater accessibility to the adsorbent surface at 50 ml cobalt solution, which would lead to a higher extent in the adsorption process. Similar type of findings has also been reported by other researchers [11,12].

3.4. Effect of pH of solution

pH plays an important role in the adsorption of metal ions by the MHApadsorbent. The species of cobalt(II) and the surface charge of the adsorbent change according to pH values. The effect of pH on the Co^{2+} adsorption was investigated by varying the pH valuein the range of 2.1–10. The MHAp exhibit a significant sorption ability (%) for Co^{2+}along all pHs used because the cobalt ions occupy the adsorption sites of the adsorbent and increase the coordination ability of the MHAp adsorbent with Co(II)[13].Our results in Fig.4 show that, the removal percentage of cobalt ions was increased with the increase in the pH values from 2.1 to 10.

It has been reported by Yuan et al., 2017[14] that cobalt (II) species are present in the forms of Co^{2+}, $Co(OH)^+$, $Co(OH)_2$, and

$Co(OH)_3^-$ at different pH values, and the predominant species are Co^{2+} for pH ≤ 8.5. The effect of the initial solution pH on the adsorption of cobalt(II) onto the UiO-66-Schiff base was investigated in the range of pH 4.0–9.0.The adsorption capacity improves with a pH from 4.0–9.0. When pH ≤ 7.0, protons could occupy most of the adsorption sites on the adsorbent surface; hence, only a little Co^{2+} could be adsorbed because of competition between Co^{2+} and protons. For pH ≥ 7.0, the protons gradually reduced such that the adsorption capacityincreased, especially at pH ≥ 8.4. The Co^{2+} would be more easily precipitated at pH ≥ 8.5 in a high concentration.

3.5. Agitation speed

Agitation speed is an important parameter for the removal of Co(II) from wastewater. To study the influence of shaking speed in batch sorption process of Co(II) was carried out in 50 ml of 7.38 ppmsolution at room temperature (20^0C) with shaking speed ranging from 70 to 300 rpm for 180 min at 0.1gMHAp adsorbent and PH ≈ 7 of the soloution. It was observed that by increasing the agitation speed of aqueous solution containing cobalt, the movement of Co(II) towards the surface of the adsorbent was also increased Fig.(5) asthe thickness of the interface was decreased and disorder in solution increased. In case of low agitation speed, active sites for adsorption remain buried inside and do not take part in sorption, resulting in poor removal efficiency [15].

3.6. Effect of the ionic strength

The influence of ionic strength on adsorption of cobalt(II) onto the MHAp adsorbent was described in Figs. 6(a) and 7(b). Apparently, the existence of NaCl, $NaNO_3$ or Na_2SO_4 generally inhibits the adsorption of Co(II) and decreased obviously. Moreover, the inhibition of adsorption capacity of Co(II) ranked as: 1.0 M > 0.1 M > 0.05 M. Generally, ionic strength basically behave in the following ways: (1) changing the structure of double electrode layer of the adsorbent; (2) reducing the radius of hydrated ions; (3) competing the activity sites with metal ions [16]. For Co(II) in this process, the third way could be primary, while the other two were secondary. The existence of Na^+ may cause steric hindrance to Co(II) due to their larger radius leading to the reduction of Co(II) adsorption capacity.

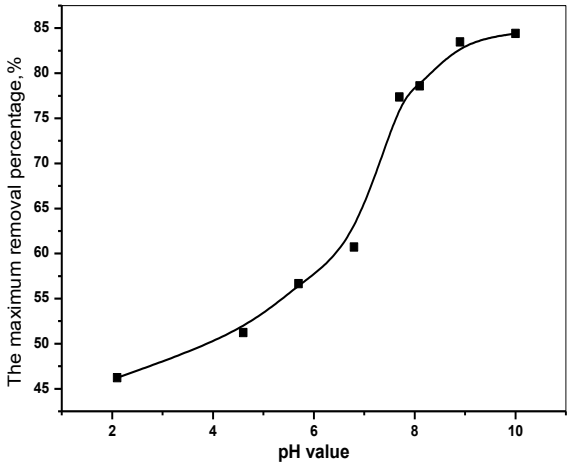

Fig. 4.Effect of the solution pH

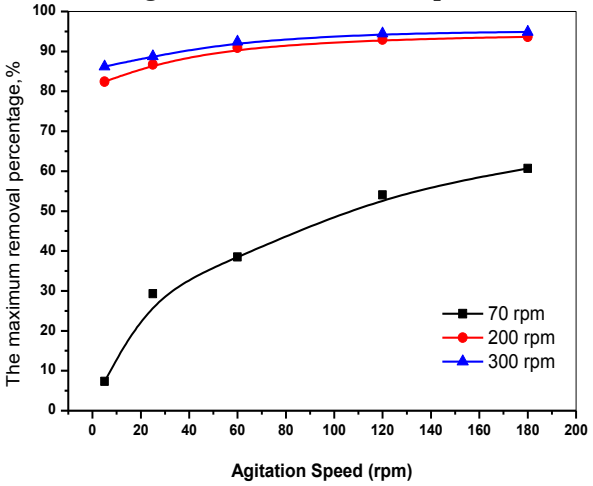

Fig. 5. Effect of the agitation speed

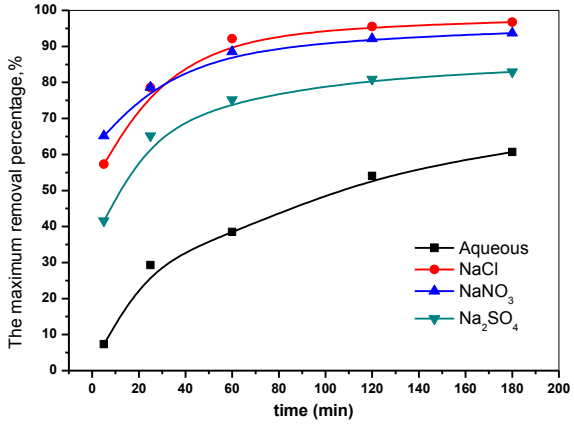

Fig.6(a). The Co(II) removal in aqueous and aqueous-inorganic systems

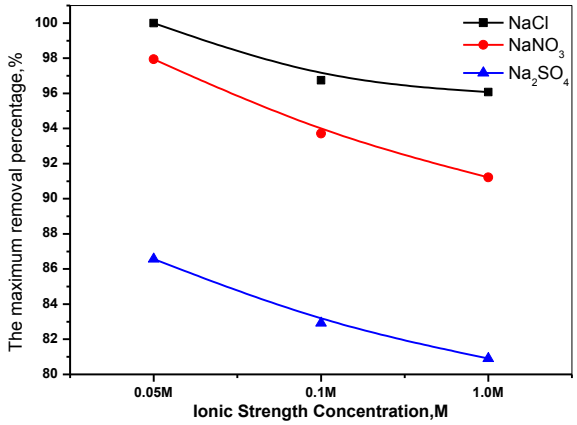

Fig.6(b). Effect of the ionic strength concentration

3.7. Adsorption isotherms

Adsorption isotherms are important for description of the interactions between the adsorbate and the adsorbent surface. The adsorption isotherm data were fitted by the four most used models: the Freundlich, Langmuir, Temkin and D-R models. The parameters obtained from the models provide important information on the sorption mechanism and the surface property and affinity of the adsorbent.

The Freundlich adsorption isotherm [17] is an empirical equation based on an exponential distribution of adsorption sites and energies. Freundlich adsorption isotherm is represented as:

$$\ln q_e = \ln KF + \frac{1}{n} \ln C_e \qquad (3)$$

where q_e is the amount of Co(II) adsorbed at equilibrium (mg g^{-1}), C_e is the concentration of Co(II) solution at equilibrium (mg l^{-1}), K_F (mg g^{-1}) and n are the Freundlich adsorption isotherm constants, being indicative of the extent of the adsorption and the degree of nonlinearity between solution concentration and adsorption, respectively. K_F value reveals the adsorption capacity of adsorbent, i.e. the greater the value of K_F, the greater adsorption capacity. The other Freundlich constant n is a measure of the deviation from linearity of the adsorption and is used to verify the type of adsorption. It is suggested that if n is equal to unity, the adsorption is linear. Furthermore, n below unity indicates that adsorption is a chemical process; while, n above unity is associated with a favourable adsorption and a physical process [18].

The Freundlich adsorption isotherm was employed to describe heterogeneous systems and reversible adsorption, not restricted to the monolayer formation. Unlike the Freundlich adsorption isotherm, the Langmuir adsorption isotherm is based on the assumption that a structure of the adsorbent is homogeneous, assuming that all sorption sites are identical and energetically equivalent.

From the plot of the experimental data based on Freundlich adsorption isotherm model, K_F and 1/n values can be calculated from intercept and slope of the linear plot between $\ln C_e$ and $\ln q_e$ (Fig. 7). The parameters K_F and n of the Freundlich adsorption isotherm for MHAp are listed in Table 1. From Table 1, it can be seen that the value of correlation coefficient (R^2) of the Freundlich adsorption isotherm is higher for Co(II) in comparison with the Langmuir adsorption isotherm. Accordingly, the adsorption process of the cobalt ions agree well withthe Freundlich adsorption isotherm model wherethe Co(II) ions adsorbed with multilayer coverage on the adsorbent surfacethrough physical bonds.Similar trends have been observed by several authors [14,19,20].

The Langmuir adsorption isotherm [21] assumes a surface with homogeneous binding sites, equivalent sorption energies, and no interaction between adsorbed species. Its mathematical form is expressed as:

$$\frac{C_e}{q_e} = \frac{1}{K_L Q_{\max}} + \frac{C_e}{Q_{\max}} \qquad (4)$$

For the Langmuir isotherm model, a dimensionless constant (R_L), commonly known as separation factor. The plot of C_e/q_e versus $C_e$for the Langmuir adsorption isotherm for Co(II): MHAp material (Fig. 8). Its slope and

intercept give the values of K_L and Q_{max} which are presented in Table 1. R_L value indicates the nature of adsorption whether it is unfavorable if $R_L > 1$, linear favorable if $R_L = 1$, favorable if $0 < R_L < 1$ and irreversible if $R_L = 0$

$$R_L = \frac{1}{1 + K_L C_0} \quad (5)$$

Where C_0 is the initial metal ions concentration and K_L is the is bonding energy of adsorption ($l\,mg^{-1}$). As can be seen, R_Ls of MHAp adsorbent was in the range $0 < R_L < 1$ indicating the favorable adsorption of Co(II).

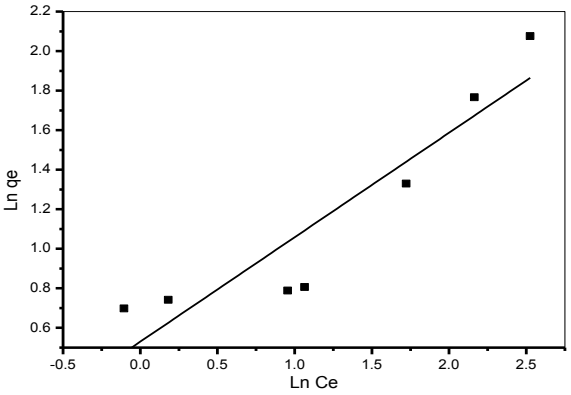

Fig.7. Freundlich plot of Co(II) adsorption

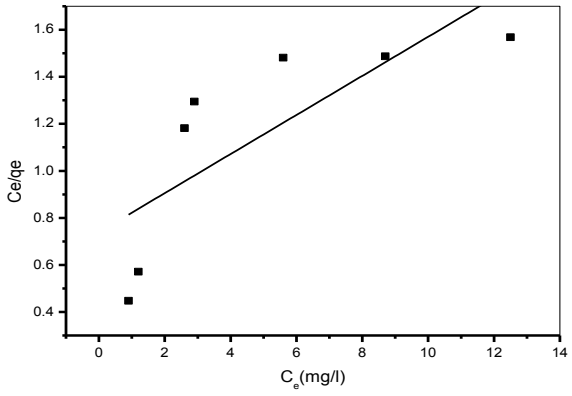

Fig.8. Langmuir plot of Co(II) adsorption

On the other hand, the correlation coefficient (R^2) for Co(II) was low in comparison with the Freundlich model. The higher value of R^2 of Freundlich model revealed that the Co(II) adsorption on MHAp material is favourable for adsorption isotherm [22].

Two other isotherm models investigated in this work were Temkin and D-R models

The Temkin isotherm model considers the indirect effect on adsorbate/adsorbate interactions on adsorption isotherm. It also assumes that the heat of adsorption of the adsorbate in the layer would decrease linearly with its coverage [23]. The linear form of the equation is given as

$$q_e = \left(\frac{RT}{b_T}\right) ln A_T + \left(\frac{RT}{b_T}\right) ln C_e \quad (6)$$

Where $B_T = \left(\frac{RT}{b_T}\right)$, B_T is the Temkin constant (J/mol) related to adsorption heat, T is the absolute temperature (K), R is the gas constant (8.314 J/mol K), and A_T is the Temkin isotherm constant (L/g). (B_T) and (A_T) can be calculated from the slopes (B_T) and intercepts (P_T ln A_T) of the plot of q_e Vs. $ln C_e$ (Fig. 9). A_T corresponds to the maximum binding energy.

The linear form of Dubinin and Radushkevich isotherm equationcan be expressed as:

$$\ln q_e = \ln (XD–R)–\beta\varepsilon^2 \quad (7)$$

ε is the polanyi potential and is equal to

$$\varepsilon = RT \ln\left(1 + \frac{1}{C_e}\right) \quad (8)$$

The value of E_{D-R} is related to the sorption mean free energy (KJ/mol). The relationship is expressed as:

$$E_{D-R} = \frac{1}{\sqrt{2\beta}} \quad (9)$$

The saturation limit X_{D-R} may represent the total specific micropore volume of the sorbent. The sorption potential is independent of the temperature, but varies according to the nature of sorbent and sorbate [24]. The slope of the plot of ln q_e versus ε^2 gives β (mol^2/J^2) and the intercept yields the sorption capacity X_{D-R} (mg/g)(Fig. 10).

Table 1. Freundlich, Langmuir, Temkin and D-R isotherm parameters for Co(II).

Freundlich			Langmiur			
n	K_f (mg/g)	R^2	Q_{max} (mg/g)	K_L (L/mg)	R_L	R^2
1.892	1.6989	0.827	12.032	0.113	0.547	0.541
Temkin			Dubinin Redushkevich (D-R)			
A_T (L/g)	B_T (J/mol)	R^2	B mol^2/J^2	X_{D-R} (mg/g)	E_{D-R} (kJ/mol)	R^2
1.746	2.107	0.742	4.7188E-07	4.638	1.03	0.316

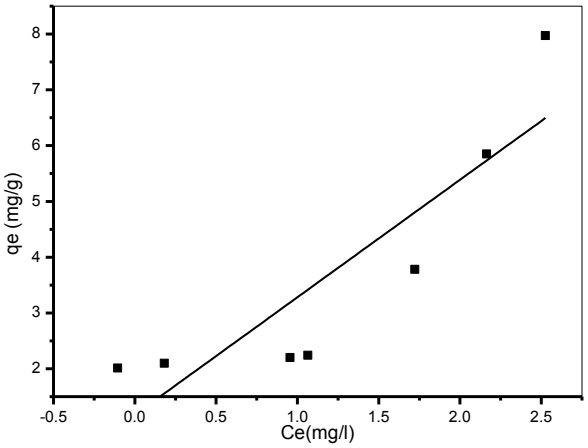

Fig.9. Temkin plot of Co(II) adsorption

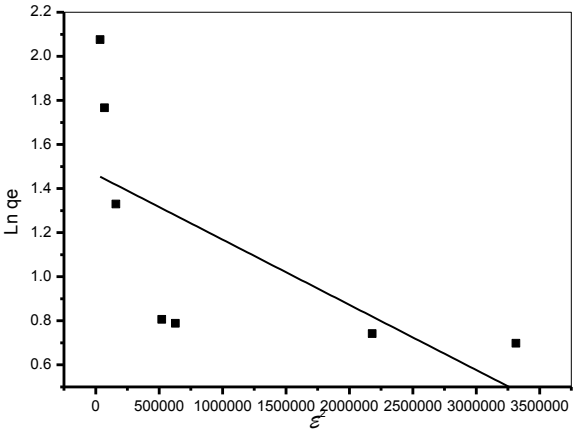

Fig.10. D-R plot of Co(II) adsorption

The sorption space in the vicinity of a solid surface is characterized by a series of equipotential surfaces having the same sorption potential. It is known that magnitude of apparent adsorption energy E_{D-R} is useful for estimating the type of adsorption and if this value is below 8 kJ/mol the adsorption type can be explained by physical adsorption, between 8 and 16 kJ/mol the adsorption type can be explained by ion exchange, and over 16 kJ/mol the adsorption type can be explained by a stronger chemical adsorption than ion exchange [25,26]. As shown in Table 1, the E_{D-R} value is 1.03 for Co(II) on the MHAp. For $E < 8$ KJ mol^{-1}, physical sorption is dominant for the adsorption mechanism. The sorption capacity X_{D-R} in the D-R equation is found to be 4.64 mg/g [27].

3.8. Effect of the contact time

The effect of contact time and the inclusion of the adsorbent on the removal of Co at 293K, 0.1 g, 7.38 ppm and 50 ml cobalt solution are presented in Fig. 6(a).It was observed that the adsorption of Co(II) was rapidly adsorbed in the first 25 min, and then the adsorption rate decreased gradually from 25 min to 120 min and finally reached an equilibrium in 180 min. This may be due to a large number of vacant surface sites available for adsorption during the initial stage of the treatment time. After a lapse of time, the remaining vacant surface sites seems hardly to be occupied due to repulsive forces between Co(II) adsorbed on the surface of MHAp and cobalt solution phase. Similar results have been reported in literature by various researchers [28,29].

3.9. Sorption kinetics

The kinetics rate of cobalt ion sorption onto MHAp was analysed using pseudo first-order, pseudo-second order, Intra-particle diffusion and the Elovich kinetic model. The agreement between experimental data and the studied models are predicted by the relatively higher correlation coefficient value (R^2).

The kinetic data were treated with the Lagergren first-order model [30] which is the earliest known one describing the adsorption rate based on the adsorption capacity. The integral form of the pseudo first-order model is generally expressed as:

$$\ln (q_e - q_t) = \ln q_{e,1,cal} - k_1 t \qquad (10)$$

The model is based on the assumption that the rate is proportional to the number of free sites or intra-particle diffusion model. If the pseudo first-order kinetics is applicable, a plot of log ($q_e - q_t$) versus t should provide a linear relationship from which $k_{1,ads}$ and predicted q_e can be determined from the slope and intercept of the plot, respectively (Fig. 11). The variation in rate should be proportional to the first power of concentration for strict surface adsorption. However, the relationship between initial solute concentration and rate of adsorption will not be linear when pore diffusion limits the adsorption process.

It was observed that first-order model failed to provide a realistic estimate of q_e of adsorbed cobalt ions since the experimental values of q_e (2.061801, 2.303086 and 0.573441 mg/g at 293, 308 and 318 K, respectively) were obtained(Table 2). On the other hand, the correlation coefficients R^2 of pseudo-first-order kinetic model were lower in comparison with R^2 values of pseudo-second-order kinetic model at 293 and 308 K with the exception of cobalt adsorption at higher temperature (318 K), suggesting that the adsorption of Co(II) ions does not follow pseudo-first-order kinetic model.

The pseudo-second-order model is based on the assumption that sorption follows a chemisorptionsmechanism. The linearized form is expressed as;

$$\frac{t}{q} = \frac{1}{k_2 q_{e,2}^2} + \frac{1}{q_{e,2}} t \qquad (11)$$

$$h = k_2 q_{e,2}^2 \qquad (12)$$

Where h(mg $g^{-1}min^{-1}$) means the initial adsorption rate, and the constants can be determined experimentally by plotting of t/q against t (Fig. 12). where k_2 is the rate constant of second-order biosorption (g/mg min).

The linearized second-order plot of t/q_t against t at three different temperatures, namely, 203, 308 and 318 Kaccording to Eq. (11) resulted in straight lines for cobalt ions which led to the determination of the second-order rate ($k_{2,ads}$) (0.0075, 0.0123 and 0.1295 at 203, 308 and 318 K, respectively). The q_e values (2.7965, 3.3320 and 3.7088 mg/gat 203, 308 and 318 K, respectively) were approximately equal to the experimental data, which indicate the appropriateness of this model(Table 2). However, the R^2 values at all temperatures used of the correlation coefficient indicated that the adsorption data for Co(II) onto MHAp best fit the pseudo-second-order model. The basic hypothesis subsequent to the pseudo-second-order model designated that chemisorptions played the most important role and may control the adsorption process [13,31-33].

Cobalt(II) ion adsorption kinetics onto MHAp adsorbent was also tested with an Elovich kinetic model. Elovich model assumes that the sorbent surface is energetically heterogeneous and that at low surface coverage, desorption or interactions between the adsorbed species will not affect the kinetics of the system [34]. The linear equation of the model is expressed as

$$q_t = \frac{1}{\beta} \ln(\alpha\beta) + \frac{1}{\beta} \ln t \qquad (13)$$

where α is the initial adsorption rate (mg/g/min), β is the desorption constant related to the extent of surface coverage and activation energy for chemisorption (g/mg). The values of model constants are determined from the slope and intercept of q_t vs lnt (Fig. 13). The comparatively less R^2 values (Table 2) obtained from this model disprove the applicability of this model for the adsorption process for the adsorbent at three different temperatures. Recorded R^2 value are relatively low (0.9818, 0.97836 and 0.81362 at 293,308 and 318 K, respectively) which indicates that the experimental data were poor fit the Elovich kinetic model. However, the intra-particle diffusion model is commonly used for

identifying the adsorption mechanism for design purposes. The effect of intraparticle diffusion resistance on adsorption can be determined by the following equation [35].

$$q_t = K_i t^{0.5} + C \qquad (14)$$

where K_i is the intercept and k_{id} is the rate constant of intraparticle diffusion (mg g^{-1} $h^{-1/2}$) which is determined from the linear plot of q_t versus $t^{1/2}$(Fig. 14), and it is usually used to compare mass transfer rates. According to this model, the plot of uptake, q_t, versus the square root of time, $t^{1/2}$ should be linear if intraparticle diffusion is involved in the adsorption process and if these lines pass through the origin, then intraparticle diffusion is the rate controlling step.

Table 2: Kinetic parameters for Co(II) adsorption in aqueous media.

	Pseudo first-order model			Pseudo second-order model			
Tem, K	qe,₁,cal mg/g	K_1 min^{-1}	R^2	qe,₂,cal mg/g	K_2 (g/mg min)	R^2	h
293	2.062	0.018	0.975	2.797	0.008	0.988	0.0590
308	٢,٣٠٣	0.024	0.977	3.332	0.012	0.997	0.1369
318	٠,٠٥٧٣	0.021	0.559	3.709	0.129	0.999	1.7817
Tem, K	Elovich model			Intraparticle diffusionmodel			
	α mg g^{-1} min^{-1}	β (g mg^{-1})	R^2	K_i	C	R^2	
293	0.1630	1.837	0.982	0.172	0.0497	0.959	
308	0.3300	1.462	0.978	0.204	0.4830	0.817	
318	825.711	3.461	0.814	0.080	2.7590	0.543	

The intra-particle diffusion rate constant and intercept values are displayed in Table 2. It was observed that the values of k_i, and ionic strength are higher for Co(II) (at 308 K) as compared to Co(II) at other temperatures (at 293 and 318 K) MHAp material. Though the intra-particle diffusion curve gives not agree with the linear fitting and does not pass through the origin. This indicates that the intraparticle diffusion is involved in the adsorption process, but not in the rate-controlling step [36-38].

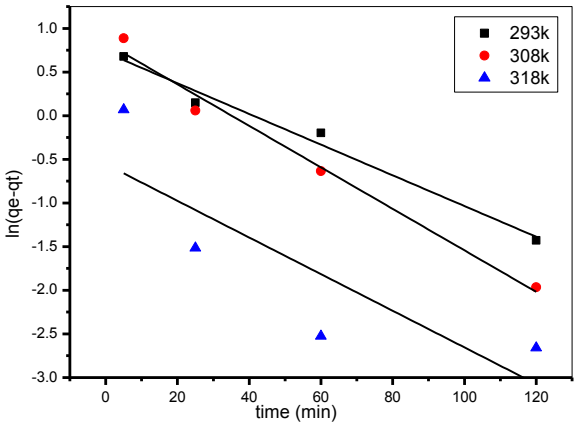

Fig.11. Pseudo-first-order plots

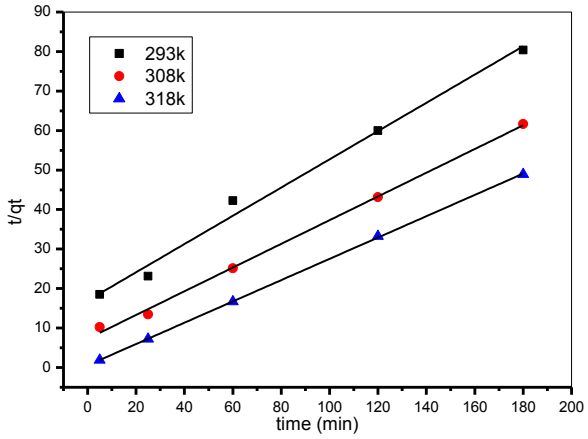

Fig.12. Pseudo-second-order plots

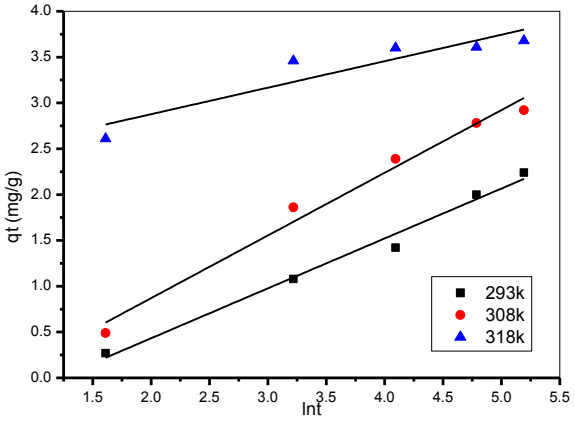

Fig.13. Elovich plots

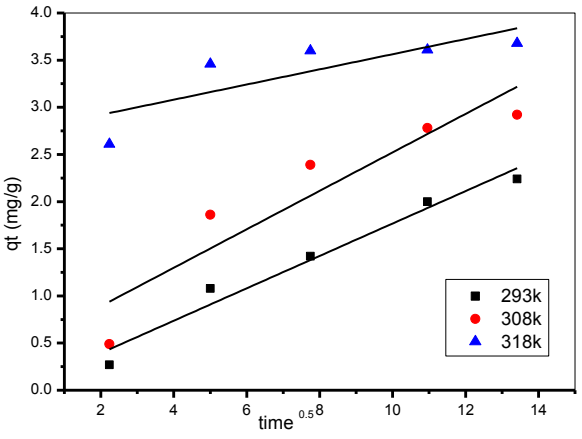

Fig.14. Intraparticle diffusion plots

3.10. Effect of temperature on adsorption process

The temperature has two major effects on the adsorption process. Increasing the temperature is known to increase the rate of diffusion of the adsorbed cobalt ions across the external boundary layer and the internal pores of the adsorbent particles, owing to the decrease in the viscosity of the solution. In addition, changing temperature will change the equilibrium capacity of the adsorbent for a particular adsorbate [39]. Fig. 15 shows the results of experiments carried out at different solution temperatures. The removal of cobalt ions increases from 2.24 to 3.68 mg/g by increasing the temperature of the solution from 293 to 318 K, indicating that the process be endothermic. This kind of temperature dependence of the amount of the cobalt adsorbed may be due to the fact that a possible mechanism of interaction is the reaction between the Co(II) ions and the cationic sites of magnetic hydroxyapatite such a reaction could be favoured at higher temperatures [40,41].

3.11. The thermodynamic parameters

To evaluate the thermodynamic feasibility and to confirm the nature of the Co(II) adsorption process on MHAp, three basic thermodynamic parameters, standard free energy (ΔG°), standard enthalpy (ΔH°), and standard entropy (ΔS°) were calculated using the following equations:

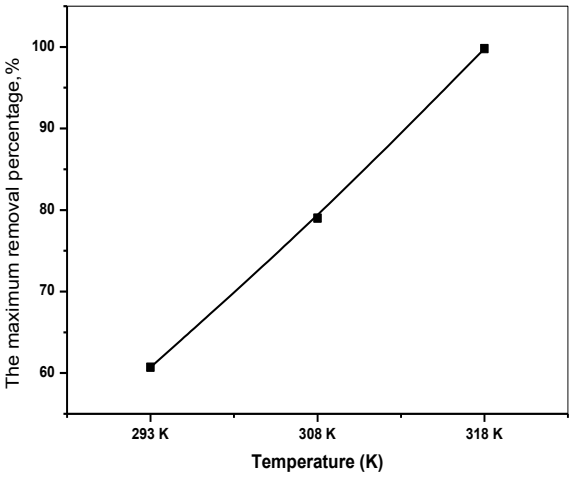

Fig. 15. Effect of the solution temperature

The Gibbs free energy change, (ΔG^o (KJ/Mol)was calculated from the following equation;

$$\Delta G^o = -RT\ln K_d \qquad (15)$$

The van't Hoff equation:

$$\ln K_d = \frac{\Delta S^o}{R} - \frac{\Delta H^o}{RT} \qquad (16)$$

The distribution coefficient (K_d) was calculated using the following equation:

$$K_d = q_e/C_e \qquad (17)$$

whereq_e (mg/g) is the amount of the metal ions adsorbed per unit mass of the MHAp and C_e(mg/l) is the concentration of the metal ions in aqueous phase, R is the universal gas constant (8.314 J mol^{-1} K^{-1}), T is the temperature in Kelvin.

The distribution coefficient (K_d) values were found to be 0.772, 1.88 and 245.33 at 293, 308, and 318 K, respectively. According to the van't Hoff equation, plot (Fig.16) of the logarithm distribution coefficient (K_d) against reciprocal temperature (1/T) results in ΔH° and ΔS° parameters. The thermodynamic parameters were listed in Table 3. The positive value of ΔG° (+0.628) for the adsorption process at low temperature (293K) shows that the process was non spontaneous in nature. On the other hand, the negative values of ΔG° for the process were -1.622 and -14.549KJ/Molat 308 and 318 K, respectively, implied that the

adsorption process was spontaneous and degree of spontaneity of reaction increased with the increasing temperature to reach -14.548 KJ/Molat 318 K. According to Bulut et al., 2008 postulation[42], the free energy change was in the range −20 to 0 KJ/Mol, referring to a major physical adsorption, while it was in the range −80 to −400 KJ/Mol, reflecting the possibility of chemical adsorption at high temperature. In our study, the value of ΔG refers to that the adsorption process was thermodynamically feasible at higher temperature. On the other hand, the positive value of ΔH° (+165.537KJ mol^{-1} K^{-1}), showing an endothermic process, and as a result, adsorption capacity increased with an increase in temperature. Moreover a positive value of ΔS° (+0.5573J mol^{-1}) showed the increased randomness at the solid-solution interface during the adsorption.

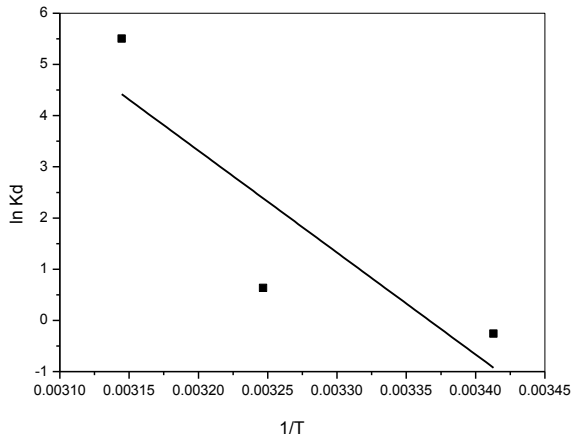

Fig.16. Van't Hoff plot

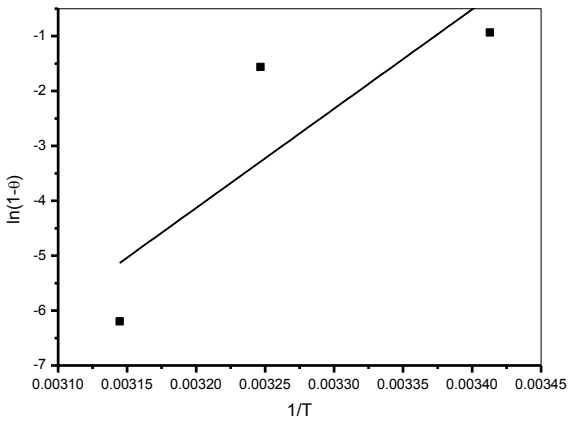

Fig.17. modified Arrheniusplot

In order to further support the assertion that physical adsorption is the predominant mechanism, the values of the activation energy (E_a) and sticking probability (S^*) were estimated from the experimental data. They were calculated using a modified Arrhenius type equation related to surface coverage (θ) [43] as expressed in equations:

$$\theta = 1 - \frac{C_e}{C_o} \qquad (18)$$

where C_0 and C_e are the initial and equilibrium metal ion concentrations, respectively

$$S^* = (1-\theta)\exp\left(\frac{E_a}{RT}\right) \qquad (19)$$

The sticking probability, S*, is a function of the adsorbate/adsorbent system under consideration and is dependent on the temperature of the system.

Combination of theEqs. (18) and (19) gives equation (20):

$$\ln\frac{Ce}{Co} = \ln S^* + \frac{E_a}{RT} \qquad (20)$$

The values of E_a and S* were obtained from the slope $\left(\frac{E_a}{R}\right)$ and intercept ln S*, respectively, of the plot of $\ln\frac{C_e}{C_o}$ vs. $\frac{1}{T}$ (Fig.17).

The parameter S* indicates the measure of the potential of an adsorbate to remain on the adsorbent indefinitely. It can be expressed as in Table3. The effect of temperature on the sticking probability was evaluated throughout the temperature range from 293 to 318 K by calculating the surface coverage at the various temperatures. Table3 also indicated that the values of $S^* \leq 1$ (1.182×10^{-27}) for the MHAp adsorbent, hence the sticking probability of the Co(II) ion onto the adsorbent are very high.

The magnitude of activation energy gives an idea about the type of adsorption which is

mainly physical or chemical. Low activation energies (<40 kJ mol^{-1}) are characteristics for physical adsorption, while higher activation energies (>40 kJ mol^{-1}) suggest chemical adsorption [44]. According to the activation energy obtained for the adsorption of cobalt onto the MHAp was 150.360 KJ/Mol indicates that the adsorption process is chemisorption. The high value of E_a suggests that the energetic barrier against the adsorption of cobalt ion is hardly to be overcome; therefore, adsorption process occurs rapidly [45].

Table 3.Thermodynamic parameters of adsorption of Co (II)in aqueous solution.

Temp. (K)	ΔS^o (J/mol. K)	ΔH^o (KJ/mol.)	R^2	ΔG^o (KJ/mol.)	S*	E_a (KJmol)	R^2
293 308 318	0.5573	165.537	0.5124	0.628 -1.622 -14.549	$1.182x\ 10^{-27}$	150.360	0.451

REFERENCES

[1] B. Krishna, P. Venkateswarlu; Indian Journal of Chemical Technology 18 (2011) 381.

[2] I.G. Shibi, T.S. Anirudhan; Chemosphere 58 (2005) 1117.

[3] A. Naeem, M.T. Saddique, S. Mustafa, S. Tasleem, K.H. Shah, M. Waseem; Journal of Hazardous Materials 172 (2009) 124.

[4] Feng Y, Gong J, Zeng G, Niu Q, Zhang H, Niu C, Deng J; Chemical Engineering Journal 162 (2010) 487–494.

[5] Hongqin X, Duilin W, Zhe J, Xiaowei L, Shouwei Z, Yan L, Cheng C; J. Radioanal Nuclear Chemistry292 (2012) 637–647.

[6] H. R. Ali, H. H. El-Maghrabi, F. Zahran, Y. M. Moustafa; Applied Surface Science 426 (2017) 56-66.

[7]Y. Wang, Q. Wei, B. Du; Journal of Colloid and Interface Science 494 (2017) 380-388.

[8] H. R. Ali, H. H. El-Maghrabi, F. Zahran, Y. M. Moustafaa; Applied Surface Science426 (2017) 56-66.

[9] S. Ben-Ali, S.Souissi-Najar, A.Ouederni; Journal of Cleaner Production154 (2017) 269-275.

[10] V. Nair, A. Panigrahy, R. Vinu; Chemical Engineering Journal 254 (2014) 491-502.

[11] J. Maity, S. K. Ray; Carbohydrate Polymers 182 (2018) 159-171.

[12] S. Duan, X. Xu, X. Liu, Y. Wanga, T. Hayatc, A. Alsaedi, Y. Meng, Jiaxing; Journal of Colloid and Interface Science 513 (2018) 92–103.

[13] S. H. Siddiqui; Groundwater for Sustainable Development6 (2018) 141-149.

[14] G.Yuan,Y.Tian, J. Liu, H. Tu, N. Liu; Chemical Engineering Journal 326 (2017) 691-699.

[15] E. Alver, M. Bulut, A. Ü. Metin, H. Çiftçi; SpectrochimicalActa Part A: Molecular and Biomolecular Spectroscopy171 (2017) 132–138.

[16] T. Wang, W.Liu, L.Xiong, N.Xu, J. Ni; Chemical Engineering Journal 215–216 (2013) 366–374.

[17] H. M. F. Freundlich; Z. The Journal of Physical Chemistry 57 (1906) 385-470.

[18] A.S. Özcan, B. Erdem, A. Özcan; Colloids and Surfaces A: Physicochemical and Engineering 266 (2005) 73-81.

[19] L. Jiang, Q. Ye, J. Chen, Z. Chen, Y. Gu; Journal of Colloid and Interface Science 513 (2018) 748–759.

[20] S.Y. Lee, H.J. Choi; Journal of Environmental Management 209 (2018) 382-392.

[21] I. Langmuir; Journal of American Chemical Society 40 (1918) 1361-1403.

[22] C. Srilakshmi, R. Saraf; Microporous and Mesoporous Materials 219 (2016) 134-144.

[23] M. J. Temkin, V. Pyzhev; ActaPhysiochim 12 (1940) 217-222.

[24] S.A. Khan, U.R. Rehman, M.A. Khan; Waste Manage 15 (1995) 271-282.

[25] S.H. Lin, R.S. Juang; Journal of Hazardous Materials92 (2002) 315-326.

[26] C.C. Wang, L.C. Juang, C.K. Lee, T.C. Hsua, J.F. Leeb, H.P. Chaob; Journal of Colloid and Interface Science 280 (2004) 27-35.

[27] T. A. E. Pehlivan; Food Chemistry132 (2012) 693-700.

[28] G. Wang, Y. Zhao, B. Yang, Y. Song; Hydrometallurgy 176 (2018) 69-72.

[29] N. Ghasemi, M. Ghasemi, S. Moazeni, P. Ghasemi, A. G. Tkachev; Journal of Industrial and Engineering Chemistry, In press 2018. http://04101crtw.1106.y.https.doi.org.mplbci.ekb.eg/10.1016/j.jiec.2018.01.008

[30] S. L. Zurtheorie der sogenannten adsorption gelosterstoffe K S V, Handlingar, 24 (1898) 1-39.

[31] L. Abramian, H. El-Rassy; Chemical Engineering Journal 150 (2009) 403-410.

[32] X. Wen, C. Du, G. Zeng, D. Huang, J. Zhang, L. Yin, S. Tan, L. Huang, H. C.G. Yu, X. Hu, CuiLai, P. Xu, J. Wan; Chemosphere 200 (2018) 173-179.

[33] F. S. Hoseinian, B. Rezai, E. Kowsari, M. Safari; Minerals Engineering119 (2018) 212-221.

[34] S. S. Gupta, K.G. Bhattacharyya; Advances in Colloid and Interface Science . 162 (1–2) (2011) 39-58.

[35] W.J. Weber, J.C. Morriss, J. Sanit; Eng. Div. American Societyof CIVIL Engineering Data Base 89 (1963) 31-60.

[36] J. Yu, C. Jiang, Q. Guan, P. Ning, J. Gu, Q. Chen, J. Zhang, R. Miao; Chemosphere 195 (2018) 632-640.

[37] V.P. Dinh, N.C. Le, L. A. Tuyene, N. Q. Hung, V.D. Nguyen, N.T. Nguyen; Materials Chemistry and Physics 207 (2018) 294-302.

[38] C. Sarkar, J. K. Basu, A. N. Samanta; Advanced Powder Technology, In press 2018, http://04101isro.1105.y.https.doi.org.mplbci.ekb.eg/10.1016/j.apt.2018.02.005

[39] Z. Al-qodah; Water Res. 34 (2000) 4295- 4303.

[40] H. Zhou, Z. Jiang, S. Wei; Applied Clay Science153 (2018) 29-37.

[41] C. S.Jayanta, K. Basu, A. N. Samanta; Advanced Powder Technologyhttps://doi.org/10.1016/j.apt.2018.02.005

[42]E. Bulut, M. İ. Özacar, A. Şengil; Microporous and Mesoporous Materials 115 (2008) 234-246.

[43] B. Singh, Das, S. K., Colloids and Surface. B: Biointer. 107 (2013) 97–106.

[44] T.S.Anirudhan, P.G. Radhakrishnan; J. Chem. Thermody., 40 (2008) 702–709.

[45] C.Sagnik, S.Chowdhury, P. D.Saha; Carbohyd. Polym. 86, (2011), 1533–1541.